(ii) The two fundamentally different processes are linked by common intermediates, which are suggested to be hydrogen-bridged complexes.

(iii) The potential energy surface of the $C_2H_5NO^{\bullet+}$ system is such that the interactions of NH_3 with ionized ketene occur in a region of the potential surface which permits CO expulsion without any hydrogen scrambling. In contrast, starting from $CH_3CONH_2^{\bullet+}$ the isomerization involves intermediates which undergo hydrogen exchange between the CH_3CO and NH_2 groups.

(iv) The enol of ionized acetamide, i.e., $CH_2{=}C(OH)NH_2^{\bullet+}$, is separated by a significant barrier from $CH_3CONH_2^{\bullet+}$.

(v) In contrast to recent suggestions,[12,13] nucleophilic substitutions involving *radical cations* are very facile. There is no experimental evidence for their "forbiddeness".

(44) While the presence of even small amounts of ion **1** ($CH_2NH_3^{\bullet+}$) in a mixture of **1** and **2** ($CH_3NH_2^{\bullet+}$) could be detected by the presence of the charge-stripping signal (m/z 31^{2+}), it is more difficult to quantitatively determine the contribution of ion **2** to the spectrum assigned for **1**. However, a detailed comparison of the spectra shown in Figure 1 leaves no doubt that ion **2** contributes at best to a minor extent only. This conclusion is supported by an independent observation. The metastable peak for CO loss from $CH_3CONH_2^{\bullet+}$ is of composite nature with a broad component ($T_{0.5}$ = 200 meV) and a narrow one ($T_{0.5}$ = 5 meV). The latter contributes to ca. 2% of the total peak area, and we assign this peak to the extrusion reaction $CH_3CONH_2^{\bullet+} \rightarrow CO + CH_3NH_2^{\bullet+}$.

Acknowledgment. Support of our work by the Deutsche Forschungsgemeinschaft, Fonds der Chemischen Industrie, Gesellschaft von Freunden der Technischen Universität Berlin, and Netherlands Organization for Pure Research (SOM/ZWO) is gratefully acknowledged. We are indebted to the Computer Center of TU Berlin for providing computer time. H.S. acknowledges helpful discussions with Profs. A. Pross and S. S. Shaik, Ben-Gurion University, Beersheba, Israel.

Magnetic-Field Effects in the Low-Temperature Polarized Emission and Absorption Spectra of Single-Crystal $[Ru(bpy)_3](PF_6)_2$

Erich Gallhuber, Gerold Hensler, and Hartmut Yersin*

Contribution from the Institut für Physikalische und Theoretische Chemie, Universität Regensburg, D-8400 Regensburg, Federal Republic of Germany. *Received December 11, 1986*

Abstract: In this paper we report on the magnetic-field dependence of the broad-band emission spectra and the zero-phonon line emission and absorption of single-crystal $[Ru(bpy)_3](PF_6)_2$ at low temperatures. It is found that a magnetic field oriented with $\mathbf{H} \perp \mathbf{c}$ induces drastic effects, whereas $\mathbf{H} \parallel \mathbf{c}$ does not change the emission and absorption properties. At T = 2 K an increase of the total emission intensity by a factor of 6 is observed under the action of a magnetic field H = 6 T. The zero-phonon lines corresponding to the two lowest excited states exhibit a Zeeman effect, the energy separation growing from 7 cm^{-1} at zero field to 13 cm^{-1} at H = 6 T. Furthermore, the magnetic field changes the (temperature-dependent) ratio of the intensities of the zero-phonon emission lines by more than two orders of magnitude up to H = 6 T, the intensity of the lower energy line increasing while that of the higher energy line decreases. In absorption only the higher energy zero-phonon line is detectable in the absence of a magnetic field. Strong magnetic fields, however, induce the lower energy absorption line and cause the same Zeeman shift as in emission. The positions of the zero-phonon lines coincide in absorption and emission. All these experimental results are explained by magnetic-field-dependent mixing of the wave functions of the two lowest excited states. A simple perturbation calculation is presented to rationalize the experimental results.

The spectroscopic properties of the $[Ru(bpy)_3]^{2+}$ complex ion (with bpy = 2,2'-bipyridine) have been studied intensively during the past two decades. In their pioneering work Crosby and coworkers set up an energy level diagram consisting of a manifold of three closely spaced levels within an energy range of about 70 cm^{-1} with fairly different photophysical properties.[1-4] Subsequently a large number of spectroscopic and theoretical investigations were performed,[5-11] but until now it has not been possible to develop a consistent model of the electronic structure of the lowest excited states.

Considerable progress concerning the characterization of the lowest excited states has been made recently by the detection of the zero-phonon emission lines in crystalline $[Ru(bpy)_3](PF_6)_2$ and $[Ru(bpy)_3](ClO_4)_2$.[12-15] In these investigations it was possible to demonstrate that polarized emission spectroscopy on single crystals of the neat material is a powerful tool in determining the photophysical properties of the excited states. On the one hand this is due to a reduction of the inhomogeneous bandwidth to a value of about 2 cm^{-1}. On the other hand, group-theoretical assignments can be accomplished on the basis of polarized spectra and optical selection rules. As a consequence it could be shown that the two very lowest excited states, which are responsible for the low-temperature emission behavior of $[Ru(bpy)_3]^{2+}$, both transform as E' (in D_3'), at least for $[Ru(bpy)_3](PF_6)_2$, although they are separated by only 7 cm^{-1}. Moreover, it was demonstrated that the second coordination sphere (i.e., the counterion) influences

(1) Harrigan, R. W.; Hager, G. D.; Crosby, G. A. *Chem. Phys. Lett.* **1973**, *21*, 487.
(2) Harrigan, R. W.; Crosby, G. A. *J. Chem. Phys.* **1973**, *59*, 3468.
(3) (a) Hager, G. D.; Crosby, G. A. *J. Am. Chem. Soc.* **1975**, *97*, 7031. (b) Hager, G. D.; Watts, R. J.; Crosby, G. A. *J. Am. Chem. Soc.* **1975**, *97*, 7037. (c) Hipps, K. W.; Crosby, G. A. *J. Am. Chem. Soc.* **1975**, *97*, 7041.
(4) Elfring, W. H.; Crosby, G. A. *J. Am. Chem. Soc.* **1981**, *103*, 2683.
(5) Felix, F.; Ferguson, J.; Güdel, H. U.; Ludi, A. *J. Am. Chem. Soc.* **1980**, *102*, 4096.
(6) Ferguson, J.; Herren, F. *Chem. Phys. Lett.* **1982**, *89*, 371.
(7) Ferguson, J.; Krausz, E. R. *Chem. Phys. Lett.* **1982**, *93*, 21.
(8) Caspar, J. V.; Meyer, T. J. *J. Am. Chem. Soc.* **1983**, *105*, 5583.
(9) Kober, E. M.; Meyer, T. J. *Inorg. Chem.* **1983**, *22*, 1614.
(10) Yersin, H.; Gallhuber, E. *J. Am. Chem. Soc.* **1984**, *106*, 6582.
(11) Yersin, H.; Hensler, G.; Gallhuber, E.; Rettig, W.; Schwan, L. O. *Inorg. Chim. Acta* **1985**, *105*, 201.
(12) Yersin, H.; Gallhuber, E.; Hensler, G. *J. Phys. (France)* **1985**, *46*, C7-453. Yersin, H.; Gallhuber, E.; Hensler, G. *Chem. Phys. Lett.* **1987**, *134*, 497.
(13) Gallhuber, E.; Hensler, G.; Yersin, H. *Chem. Phys. Lett.* **1985**, *120*, 445.
(14) Hensler, G.; Gallhuber, E.; Yersin, H. *Inorg. Chim. Acta* **1986**, *113*, 91.
(15) "XI IUPAC Symposium on Photochemistry"; Hensler, G.; Gallhuber, E.; Yersin, H. *Volume of Abstracts*; Lisbon, 1986; p 382.

0002-7863/87/1509-4818$01.50/0

the energy separations of the emitting states, the absolute energies of the transitions, and the radiative rates. Thus, considerable new information was gained from these single-crystal investigations.

In this paper we continue our work concerning the spectroscopic properties of crystalline $[Ru(bpy)_3]^{2+}$ compounds by reporting the magnetic-field effects on the low-temperature polarized absorption and emission of single-crystal $[Ru(bpy)_3](PF_6)_2$. A qualitative model is presented to rationalize the observed magnetically induced changes in the emission and absorption spectra and thereby extending a preliminary report given earlier.[16]

Experimental Section

$[Ru(bpy)_3](PF_6)_2$ was prepared and crystals were grown as described previously.[10,14] Hexagonal needles of good optical quality were mounted over a hole in a copper strip and placed between the solenoids of an Oxford SM 4 superconducting magnet. The cryostat of the probe chamber can be operated either as a bath or as a boil-off cryostat. The direction of the magnetic field was always perpendicular to the direction of detection. Luminescence was excited by the UV and visible lines from a Coherent Innova 90 Ar^+ laser or by the 543.5-nm line of a He–Ne laser. Incident power levels were held well below 1 mW to avoid sample heating. Checks on the sample temperature were easily performed below 4.2 K with the help of the temperature-dependent intensity ratio of the zero-phonon lines of single-crystal $[Ru(bpy)_3](PF_6)_2$.[14] The microspectrophotometer for polarized absorption and emission measurements has already been described in detail.[17] Luminescence was dispersed by a Spex 1404 double monochromator, detected by a cooled EMI 9659 QB photomultiplier tube with an extended-red S20 photocathode, and recorded with use of a PAR SSR 1105 photon counter and a chart recorder. Emission spectra were not corrected for the spectral response of the detection system. The monochromator readout was calibrated to ±1 cm^{-1} with a low-pressure mercury lamp. For the highly resolved spectra, resolution was about 1 cm^{-1}. Specific care was taken to neither illuminate nor detect emission from crystal edges or crystal imperfections possibly introduced by the low temperatures in order to avoid polarization scrambling.

Results

Magnetic-field effects on the low-temperature polarized emission and absorption of single-crystal $[Ru(bpy)_3](PF_6)_2$ were measured for two magnetic-field directions for both the broad bands and the zero-phonon lines at T = 2 and 4.5 K. The magnetic-field dependence of the spectra was found to be independent both of the method of growing the samples and of the exciting wavelengths. Figure 1 shows the $\mathbf{E}\perp\mathbf{c}$-polarized broad-band emission at T = 2 K for several magnetic-field strengths with the magnetic field oriented perpendicular to the **c** axis of the crystal needle (i.e., $\mathbf{E}\|\mathbf{H}$). In Figure 2 the magnetic-field dependence of the zero-phonon lines both in emission and absorption with $\mathbf{H}\perp\mathbf{c}$ and $\mathbf{E}\|\mathbf{H}$ is reproduced for T = 2 K. The magnetic-field behavior of the zero-phonon line emission at T = 4.5 K is presented in Figure 3.

At T = 2 K, two maxima at about 17 250 cm^{-1} (band I) and 17 600 cm^{-1} (band II) are observed in the absence of a magnetic field (see Figure 1). Application of the magnetic field produces a grow in of the blue band II accompanied by a steady increase in total intensity (see Figure 4). At T = 4.5 K the broad-band spectrum has its maximum already at 17 600 cm^{-1} without magnetic field; thus no magnetic-field induced spectral change is obtained and the total intensity increases only by a factor of 2 up to H = 6 T (see Figure 4). The magnetic-field behavior is nearly the same for the $\mathbf{E}\|\mathbf{c}$- ($\mathbf{E}\perp\mathbf{H}$) polarized broad-band spectra, but all emission intensities are weaker by a factor of at least 10.

The magnetic-field effects are still more drastic for the zero-phonon emission lines. From Figures 2 and 3 it is seen that under the influence of a magnetic field $\mathbf{H}\perp\mathbf{c}$ the $\mathbf{E}\perp\mathbf{c}$-polarized emission intensity of line II decreases rapidly, whereas line I gains considerable intensity. The intensity ratio of the two lines $I_{\text{line II}}/I_{\text{line I}}$ at T = 4.5 K falls from a value of 20 without magnetic field to 0.04 at H = 6 T (see Figure 5). Furthermore, the two lines move apart under the action of the magnetic field, the energy separation almost doubling by H = 6 T (see Figure 6). For the $\mathbf{E}\|\mathbf{c}$-polarized line emission the effects are the same but the intensities are generally weaker by a factor of 20 to 40, which might

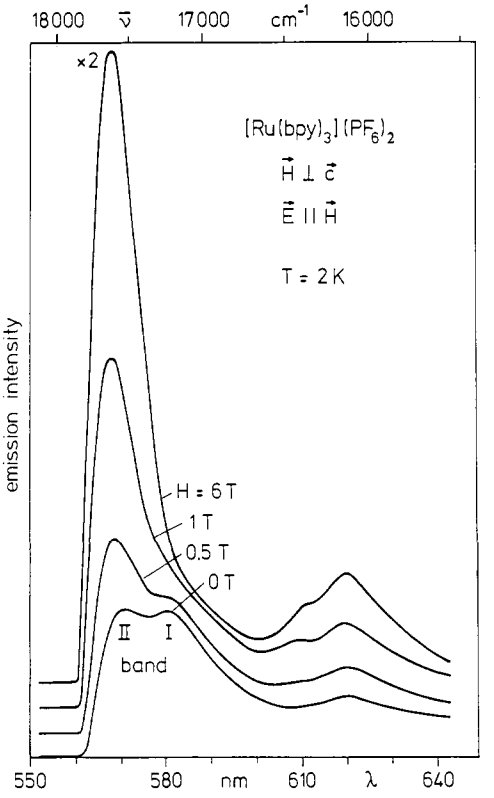

Figure 1. Broad-band emission spectra of single-crystal $[Ru(bpy)_3](PF_6)_2$ at T = 2 K for various magnetic-field strengths. The magnetic field **H** is oriented perpendicular to the crystallographic **c** axis (needle axis of the crystal). Polarized emission is detected with $\mathbf{E}\|\mathbf{H}$ ($\mathbf{E}\perp\mathbf{c}$). The intensities of the $\mathbf{E}\|\mathbf{c}$- ($\mathbf{E}\perp\mathbf{H}$) polarized spectra are weaker by a factor of at least 10. Note that the spectra for H = 6 T has to be multiplied by the given factor to be comparable.

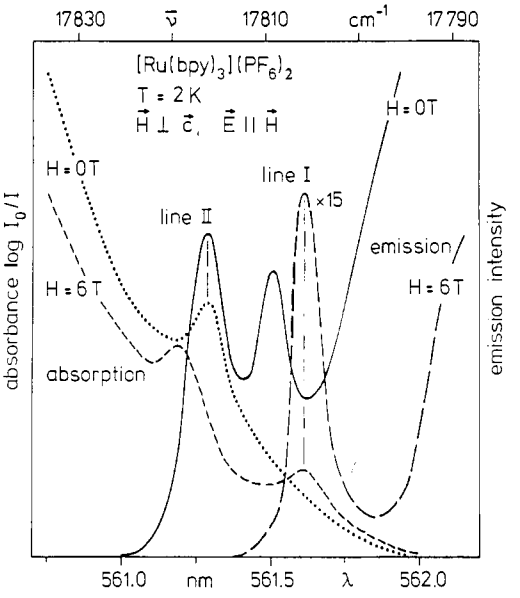

Figure 2. Zero-phonon absorption and emission lines of single-crystal $[Ru(bpy)_3](PF_6)_2$ at T = 2 K without magnetic field and with H = 6 T, orientation $\mathbf{H}\perp\mathbf{c}$. Polarized absorption and emission is detected with $\mathbf{E}\|\mathbf{H}$. The intensities and absorbances of the corresponding $\mathbf{E}\|\mathbf{c}$- ($\mathbf{E}\perp\mathbf{H}$) polarized spectra are weaker by a factor of at least 20. Note that the Zeeman shift is the same in absorption and emission. The energetical positions of the corresponding lines coincide in absorption and emission within ±0.5 cm^{-1} (experimental error). The emission spectrum for H = 6 T has to be multiplied by the given factor to be comparable in intensity to the zero-field spectrum.

(16) "XI IUPAC Symposium on Photochemistry"; Gallhuber, E.; Hensler, G. Yersin, H. *Volume of Abstracts*; Lisbon, 1986; 384.
(17) Yersin, H.; Gliemann, G. *Messtechnik (Braunschweig)* **1972**, *80*, 99.

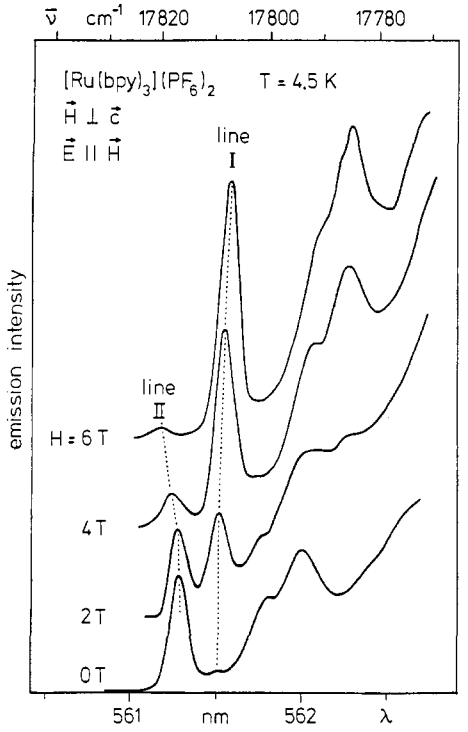

Figure 3. Zero-phonon emission lines of single-crystal $[Ru(bpy)_3](PF_6)_2$ at $T = 4.5$ K for various magnetic field strengths. The magnetic field is oriented with $\mathbf{H} \perp \mathbf{c}$. Polarized emission is detected with $\mathbf{E} \parallel \mathbf{H}$. The intensities of the corresponding $\mathbf{E} \parallel \mathbf{c}$- ($\mathbf{E} \perp \mathbf{H}$) polarized spectra are weaker by a factor of at least 20.

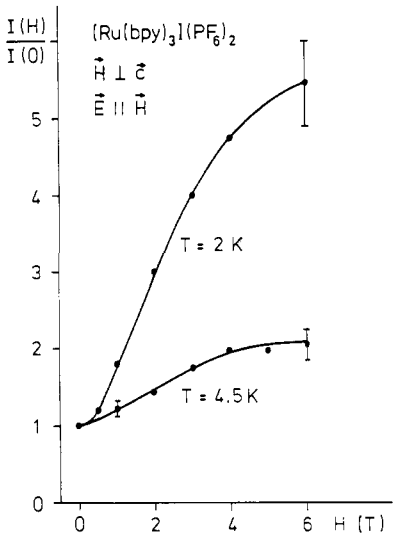

Figure 4. Magnetic-field dependence of the total $\mathbf{E} \parallel \mathbf{H}$-polarized emission intensity $I(H)$. The intensity at a magnetic field strength H has been normalized to the zero-field intensity.

result from polarization scrambling.

The zero-phonon line absorption is also affected by strong magnetic fields oriented with $\mathbf{H} \perp \mathbf{c}$ (see Figure 2). Whereas without a magnetic field only the zero-phonon line II can be detected in absorption, with a magnetic field applied line I is seen to grow in in absorption, too. Simultaneously, the extinction coefficient of line II decreases slightly and the energy separation of the two absorption lines increases, paralleling the effect seen in emission. At $H = 6$ T the ratio of the extinction coefficients of the two zero-phonon lines reaches the value 1.1.

A magnetic field oriented parallel to the crystal needle axis produces only very small effects identical with those observed for $\mathbf{H} \perp \mathbf{c}$ at low magnetic-field strengths. As the magnetic-field dependence of the intensity ratio of the zero-phonon lines (which is a sensitive measure of the magnetic-field strength for $\mathbf{H} \perp \mathbf{c}$ at

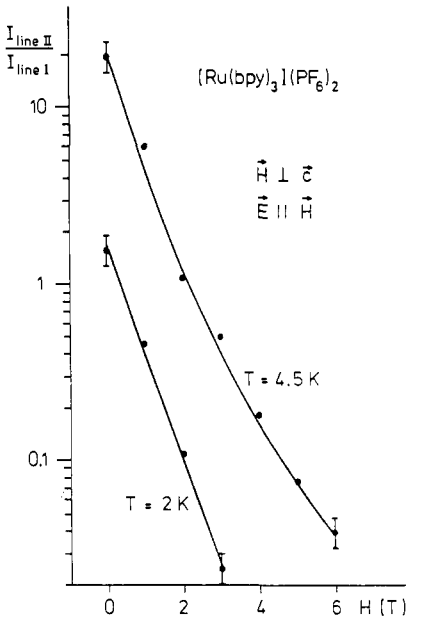

Figure 5. Magnetic-field dependence of the intensity ratio of the two zero-phonon emission lines. In determining the intensities of the two lines the broad-band background was subtracted. Note that the ordinate has a logarithmic scale.

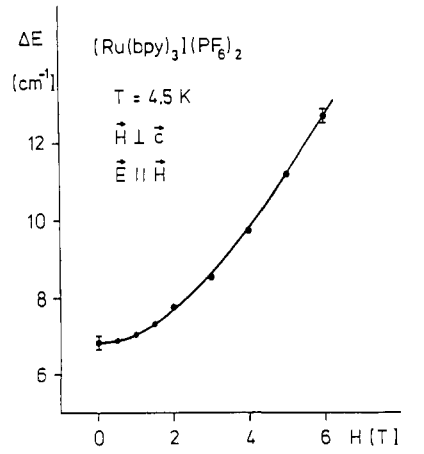

Figure 6. Magnetic-field dependence of the energy separation ΔE of the two zero-phonon emission lines at $T = 2$ and 4.5 K. The experimental points represent the mean values of three measurements.

fixed temperature) was slightly different for each experiment, we conclude that this behavior is due to small misalignments of the crystal needles which respect to the magnetic-field orientation. For example, at $H = 6$ T ($\mathbf{H} \parallel \mathbf{c}$) a misalignment by 5° leads to an effective magnetic field strength of $H \approx 0.5$ T perpendicular to the needle axis sufficient to induce the observed effects.

Discussion

For temperatures below 10 K, the spectroscopic properties of single-crystal $[Ru(bpy)_3](PF_6)_2$ are determined by the two lowest excited states that have been assigned previously to triplet components of 4d(Ru) → π*(bpy) character.[1-14] These two states are separated by only (6.9 ± 0.1) cm^{-1}, but the radiative transition from the very lowest excited state 1E′ is more forbidden by a factor of about 200 than that from the second lowest one, 2E′. As emission from both states is totally $\mathbf{E} \perp \mathbf{c}$-polarized, they were both assigned to E′ in D_3'.[10,12,14] This assignment is supported by a recent report on ODMR signals obtained at $T = 1.4$ K,[20] which shows that the two states are really degenerate. The corresponding zero-phonon lines at 17 809 cm^{-1} ≙ 561.5 nm (line I in Figures 2 and 3) and at 17 816 cm^{-1} ≙ 561.3 nm (line II) have been detected in emission[12,14] as well as in absorption and excitation spectra (only line II).[18] In contrast, Krausz and Nightingale were

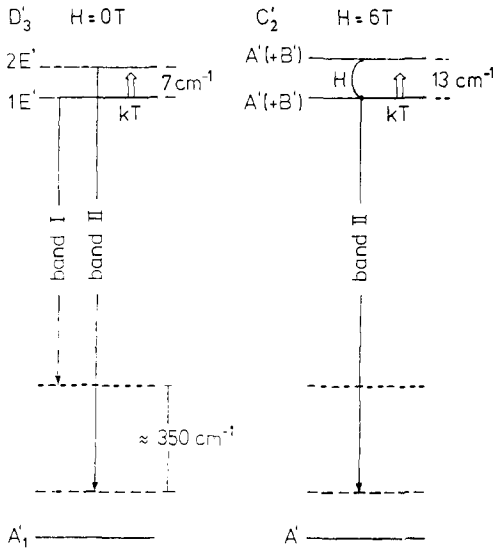

Figure 7. Simplified energy level diagram for the two lowest excited states showing the effect of a high magnetic field on the broad-band emission. The situation depicted is for $T \approx 2$ K: Without magnetic field the broad-band transitions (bands I and II) from both states involving different intramolecular vibrations are seen. For the two states magnetically coupled, emission occurs mainly from the lower state with the emission properties of the higher lying state.

unable to detect the zero-phonon absorption line because of the thickness of their crystal.[19] Considering the parallelism in the temperature development of the zero-phonon lines and the broad-band spectra (intensities, polarization, activation energies), there is little doubt that the zero-phonon lines really represent the purely electronic transitions of the $[Ru(bpy)_3]^{2+}$ chromophores (for further detailed arguments see ref 14 and 18). Even when resonant energy transfer is taken into account this conclusion remains valid.[18]

We now turn to the interpretation of the magnetic-field effects. As has already been discussed by Crosby et al. for $[Ru(bpy)_3]^{2+}$ doped into $[Zn(bpy)_3]SO_4 \cdot 7H_2O$,[21] the magnetic-field effect on the low-temperature emission can be explained by a magnetic-field induced mixing of the wave functions of the two lowest excited states. Group theory tells us that they might mix under the action of a symmetry-lowering magnetic field whatever its orientation is, because the two states transform equally in the parent group (D_3'). Actually a magnetic field oriented with $\mathbf{H} \| \mathbf{c}$ does *not* lead to effects that could be interpreted this way. Appearently the electronic structure of the two lowest states prevents them from being coupled by a magnetic field $\mathbf{H} \| \mathbf{c}$. This result points to distinct properties of the wave functions. While this might be valuable information needed to develop the wave functions, we are not able to substantiate this point further.

On the contrary, drastic effects are obtained for $\mathbf{H} \perp \mathbf{c}$. A magnetic field with this orientation lowers the symmetry from D_3' to C_2'. Thus the E' states may split into A' and B', the ground state remaining totally symmetric (A'). The selection rules for electric dipole transitions in C_2' are as follows: A' $\leftrightarrow$ A' allowed for $\mathbf{E} \| \mathbf{H}$, B' $\leftrightarrow$ A' allowed for $\mathbf{E} \perp \mathbf{H}$. Realizing the geometry used, i.e., the orientation of the magnetic field perpendicular to the direction of detection, only emission from the A' component of an E' state can be observed with a crystal needle. For the observation of the $\mathbf{E} \perp \mathbf{c}$- ($\mathbf{H} \perp \mathbf{c}$) polarized B' emission resulting from the splitting of an E' state, axial crystals are necessary, which, however, could not be obtained of sufficient quality to allow polarized emission measurements.

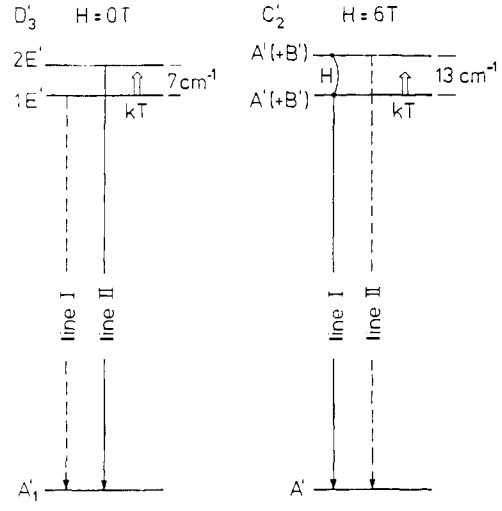

Figure 8. Simplified energy level diagram for the two lowest excited states showing the effect of the high magnetic field on the zero-phonon emission lines. The situation depicted is for $T \approx 4.5$ K: Without magnetic field line II is dominant, whereas by magnetic-field induced mixing of the two states line I becomes the more intense line.

The situation we will now explain is shown schematically in Figure 7. At $T = 2$ K emission from the two states occurs with nearly equal intensities. This results from the balance between the Boltzmann factor (which is determined by the energy separation and the ambient temperature) and the ratio of the radiative rates k_{2r}/k_{1r} corresponding to the transitions from the two lowest excited states. A magnetic field applied with $\mathbf{H} \perp \mathbf{c}$ mixes the wave functions of the two states. As a consequence, the lower state borrows the radiative properties of the higher-lying state (spectral band shape and radiative rate of the corresponding transition). Thus the total emission intensity increases (Figures 1 and 4), and under the action of the magnetic field the band shape approaches the contour at higher temperatures. Even for $T = 4.5$ K a slight magnetically induced intensity increase is observed (Figure 4). It is clear that the difference of about 10 cm^{-1} in the absolute energies of the two states cannot be observed in the broad-band spectra.

Figure 8 shows schematically the situation for a qualitative description of the influence of a magnetic field on the zero-phonon lines. For increasing magnetic-field strengths line I grows in while line II decreases in intensity for two reasons: First, line I grows in to the extent that the lower state receives the allowedness of the upper state through the mixing of the wave functions. Second, by the action of the Zeeman effect (see Figure 6) the decreasing Boltzmann factor favors population of the lower state. Therefore, at $T = 4.5$ K the intensity ratio of the zero-phonon lines is expected to change quite drastically. Indeed, it is found by experiment that the ratio is reduced from a value of about 20 to about 0.04, that is by more than two orders of magnitude (see Figure 5).

In order to calculate the extent of the mixing of the wave functions, we first evaluate the magnetic-field dependence of the ratio of the radiative rates k_{2r}/k_{1r} for the transitions from two lowest excited states. The ratio of the total emission intensities I_2/I_1 is given by

$$\frac{I_2}{I_1}(H) = \frac{k_{2r}}{k_{1r}}(H) \exp[-\Delta E(H)/kT] \qquad (1)$$

It is impossible to determine the ratio of the intensities I_2/I_1 from the broad-band spectra, as the corresponding spectral bandshapes and the energy positions are the same (within 10 cm^{-1}) when a magnetic field is applied. The situation encountered with the zero-phonon lines is much more favorable, because they are spectrally well separated and their intensities can be determined quite easily. Moreover, the magnetic-field effect on the zero-phonon emission lines can be traced clearly in a relatively large

(18) Yersin, H.; Hensler, G.; Gallhuber, E. *Inorg. Chim. Acta* **1987**, *132*, No. 2. Gallhuber, E.; Hensler, G.; Yersin, H. In *Proceedings of the Seventh International Symposium on Photochemistry and Photophysics of Coordination Compounds*; Yersin, H., Vogler, A., Eds.; Springer-Verlag: Heidelberg, 1987.

(19) Krausz, E.; Nightingale, T. *Inorg. Chim. Acta* **1986**, *120*, 37.

(20) Yamauchi, S.; Komada, Y.; Hirota, N. *Chem. Phys. Lett.* **1986**, *129*, 197.

(21) (a) Watts, R. J.; Harrigan, R. W.; Crosby, G. A. *Chem. Phys. Lett.* **1971**, *8*, 49. (b) Baker, D. C.; Crosby, G. A. *Chem. Phys.* **1974**, *4*, 428.

temperature range (up to $T \approx 10$ K), while the magnetically induced intensity increase in the broad-band spectra becomes rather faint as temperature increases above $T \approx 2$ K. Assuming that the electron–phonon coupling strengths for the two states are equal and not very dependent on the magnetic field, we may replace the total emission intensities by the intensities of the zero-phonon lines, which yields

$$\frac{k_{2r}}{k_{1r}}(H) = \frac{I_{\text{line 11}}}{I_{\text{line 1}}}(H) \exp[\Delta E(H)/kT] \qquad (2)$$

Thus, by use of the results of Figures 5 and 6, the plot of Figure 9 is obtained. It is seen that the magnetic-field-dependent ratio of the radiative rates k_{2r}/k_{1r} falls sharply from a value of 210 ± 20 at zero field to ≈2 at $H = 6$ T. Independently, the ratio of the radiative rates can be deduced from the absorption spectra. A value of about 1.1 is obtained for $H = 6$ T. These two values for the ratio of the radiative rates at $H = 6$ T seem to be quite consistent considering the assumptions introduced.

In the following analysis we want to estimate the amount of the mixing of the wave functions by a simple perturbation approach employing a two-state model. We believe that a two-state model is appropriate, because the third excited state lies about 50 cm^{-1} above the lowest one,[10] approximately seven times the separation of the two lowest excited states. Its contribution to the mixing should be negligible within limits of this estimate, since the mixing goes as the square of the inverse of the separation (see below). In this first-order treatment of the perturbation caused by the magnetic field we follow closely the route described by Gliemann and co-workers.[22,23] The perturbed wave functions $|1\rangle_H$ and $|2\rangle_H$ are obtained from the unperturbed wave functions $|1\rangle$ and $|2\rangle$ by

$$|1\rangle_H = \alpha|1\rangle + \beta|2\rangle \qquad |2\rangle_H = \alpha|2\rangle - \beta|1\rangle \qquad (3)$$

with the mixing coefficient

$$\beta = \mu_B H \frac{\langle 2|\mathbf{L} + 2\mathbf{S}|1\rangle}{|E_2 - E_1|} \qquad (4)$$

which is proportional to the magnetic-field strength H, and with the normalization condition

$$\alpha^2 + \beta^2 = 1 \qquad (5)$$

Thus, the ratio of the radiative rates is

$$\frac{k_{1r}}{k_{2r}}(H) = \frac{|\alpha\langle 1|\mu|0\rangle + \beta\langle 2|\mu|0\rangle|^2}{|\alpha\langle 2|\mu|0\rangle - \beta\langle 1|\mu|0\rangle|^2} \qquad (6)$$

where μ is the electric dipole operator and $|0\rangle$ denotes the wave function of the ground state. For $[Ru(bpy)_3](PF_6)_2$ the matrix element $\langle 1|\mu|0\rangle$ is much smaller than $\langle 2|\mu|0\rangle$, and we may drop $\beta\langle 1|\mu|0\rangle$ in the denominator for low magnetic-field strengths. Thus we arrive at

$$\frac{k_{1r}}{k_{2r}}(H) - \frac{k_{1r}}{k_{2r}}(0) \approx \frac{\beta^2}{\alpha^2} = \frac{\beta^2}{1 - \beta^2} \qquad (7)$$

having neglected the factor $(2\beta/\alpha)\langle 1|\mu|0\rangle\langle 2|\mu|0\rangle$ on the right-hand side. For low magnetic fields, where $\beta^2 \ll 1$, we find that expression 7 is proportional to the square of the magnetic field strength, H^2.

A plot of $k_{1r}/k_{2r}(H) - k_{1r}/k_{2r}(0)$ vs. H^2 (deduced from Figure 9) is drawn in Figure 10. As can be seen, a straight line is obtained up to fairly strong magnetic fields. Thus we may conclude that our simple perturbation approach allows us to describe the magnetic-field-induced mixing of the wave functions quite well. Further, using (7) we can estimate the extent to which the wave functions are mixed at high magnetic fields. We find that at H = 6 T the wave functions of the two lowest excited states of $[Ru(bpy)_3](PF_6)_2$ consist only of about two-thirds of their unperturbed wave functions, whereas about one-third is admixed from their counterparts.

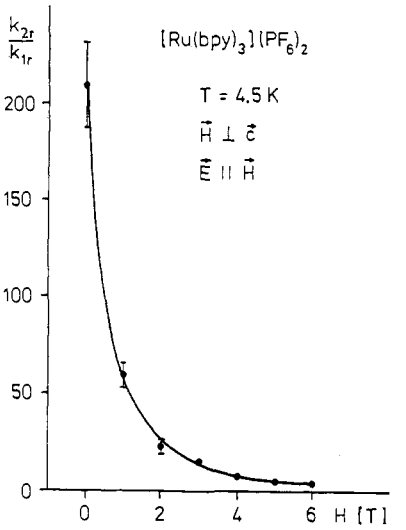

Figure 9. Magnetic-field dependence of the ratio of the radiative rates k_{2r}/k_{1r} for the transitions from the two lowest excited states. The ratio was calculated by using expression 2. Error bars represent experimental but not systematical errors.

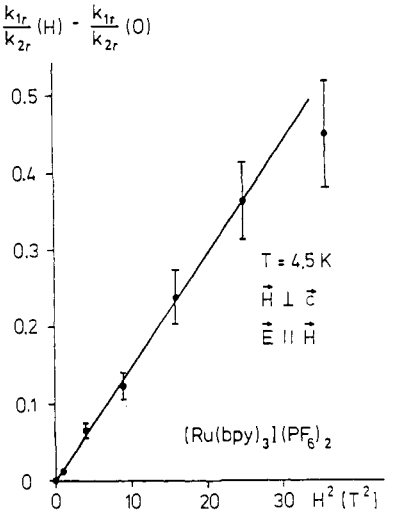

Figure 10. Magnetic-field dependence of the difference of the ratios of the radiative rates k_{1r}/k_{2r} with and without magnetic field, plotted vs. the square of the magnetic-field strength.

Conclusion

The magnetic-field effects on the low-temperature emission and absorption spectra of $[Ru(bpy)_3](PF_6)_2$ are consistently explained by a magnetically induced mixing of the wave functions of the two lowest excited states. The parallelism of the magnetic-field dependence of the zero-phonon emission lines and the broad-band spectra is a further indication that in single-crystal $[Ru(bpy)_3](PF_6)_2$ the emission spectra at low temperatures reflect intrinsic properties of the complex ion. Moreover, any presumption that the zero-phonon lines and the broad-band spectra could not be produced by the same type of chromophores is excluded.

Acknowledgment. The authors express their thanks to Prof. G. Gliemann for generous support of this work. Financial grants by the Studienstiftung des Deutschen Volkes, the Deutsche Forschungsgemeinschaft, the Stiftung Volkswagenwerk, and the Verband der Chemischen Industrie are gratefully acknowledged.

Registry No. $[Ru(bpy)_3](PF_6)_2$, 60804-74-2.

(22) Hidvegi, I.; v. Ammon, W.; Gliemann, G. *J. Chem. Phys.* **1982**, *76*, 4361.
(23) Gliemann, G. *Comments Inorg. Chem* **1987**, *5*, 263.